

Effect of Microencapsulated Curing Agents on the Curing Behavior for Diglycidyl Ether of Bisphenol A Epoxy Resin Systems

Hongxia Xu, Zhengping Fang, Lifang Tong

Institute of Polymer Composites, Zhejiang University/Key Laboratory of Macromolecular Synthesis and Functionalization, Hangzhou 310027, People's Republic of China

Received 24 February 2007; accepted 4 June 2007

DOI 10.1002/app.26972

Published online 23 October 2007 in Wiley InterScience (www.interscience.wiley.com).

ABSTRACT: Microcapsules containing a curing agent, 2-phenyl imidazole (2PZ), for a diglycidyl ether of bisphenol A (DGEBA) epoxy resin were prepared by a solid-in-oil-in-water emulsion solvent evaporation technique with poly(methyl methacrylate) (PMMA) as a polymeric wall. The mean particle size of the microcapsules and the concentration of 2PZ were about 10 μm and nearly 10 wt %, respectively. The onset cure temperature and peak temperature of the DGEBA/2PZ-PMMA microcapsule system appeared to increase by nearly 30 and 10 $^{\circ}\text{C}$, respectively, versus those of the DGEBA/2PZ system because of the increased reaction energy of curing. The former could take more than 3 months at room temperature, whereas the latter was cured after only a week. The values of the reaction order (a curing kinetic parameter) for DGEBA/2PZ and

DGEBA/2PZ-PMMA microcapsules were quite close, and this showed that the curing reactions of the two samples proceeded conformably. The curing mechanism was investigated, and a two-step initiation mechanism was considered: the first was assigned to adduct formation, whereas the second was due to alkoxide-initiated polymerization. The glass-transition temperature of DGEBA/2PZ was 165.2 $^{\circ}\text{C}$, nearly 20 $^{\circ}\text{C}$ higher than the glass-transition temperatures of DGEBA/2PZ-PMMA microcapsules and DGEBA/2PZ/PMMA microspheres, as determined by differential scanning calorimetry measurements. © 2007 Wiley Periodicals, Inc. *J Appl Polym Sci* 107: 1661–1669, 2008

Key words: curing of polymers; kinetics (polym.); microencapsulation

INTRODUCTION

Epoxy resins have good thermal and dimensional stability, excellent chemical and corrosion resistance, high tensile strength and modulus, and ease of handling and processability, which ensure their widespread applications in the aerospace and electronic industries in the forms of structural adhesives, advanced composite matrices, and packaging materials.^{1,2} Such excellent properties are not displayed by epoxy resins until they are cured by a certain kind of curing agent under certain conditions and are turned into networks. The properties of cured epoxy polymers depend not only on the nature of the chemical structure of the starting resins³ but also on the molecular structure of the curing agents and their forms in epoxy resins.⁴ For some practical purposes, epoxy resins are required to be stable during storage and to be cured when they are needed; this leads to the birth of latent curing agents, including the microencapsulation of curing agents.

In semiconductor devices,^{5,6} adhesive-fastened pad-eye devices,⁷ and one-part curable epoxy adhesives stable at the ambient temperature,⁸ ambient-temperature-stable and fast-cure properties are needed because epoxy resin systems should be stored and transported stably at a low temperature for a quite long time. The shelf life of an epoxy-resin-based system containing microencapsulated curing agents is prolonged through the separation of the curing agents from the epoxy resin during storage. When the temperature increases to a desired point, the capsules are broken, and the curing agents are liberated to cure the epoxy resin. Successful microcapsules containing modified imidazole were prepared through an interfacial polymerization process in Xing et al.'s work,⁴ and an obvious delay in the curing reaction was observed. Cao et al.⁶ showed that the initial curing temperature for a resin system containing a microencapsulated curing agent was increased by about 50 $^{\circ}\text{C}$ versus that of a sample containing nonencapsulated hardeners. The shelf life was prolonged successfully. Obviously, from a practical standpoint, the polymers used to encapsulate the curing agents of an epoxy resin should possess a controllable softening point or suitable decomposition temperature, in addition to good compatibility with the epoxy resin. Suitable wall materials and

Correspondence to: L. Tong (lftong@zju.edu.cn).

Contract grant sponsor: National Natural Science Foundation of China; contract grant number: 50473036.

Journal of Applied Polymer Science, Vol. 107, 1661–1669 (2008)
© 2007 Wiley Periodicals, Inc.

TABLE I
Constituents of the Samples Characterized
with Scanning DSC

| Sample | DGEBA (g) | 2PZ (g) | PMMA microspheres (g) | 2PZ/PMMA microcapsules (g) |
|--------|--------------|------------|--------------------------|-------------------------------|
| a | 100 | 0 | 18 | 0 |
| b | 100 | 2 | 0 | 0 |
| c | 100 | 0 | 0 | 20 |
| d | 100 | 2 | 18 | 0 |

The concentration of 2PZ in the 2PZ/PMMA microcapsules, determined by TGA, was 10 wt %.

core curing agents have been reported in a patent.⁹ Examples of wall materials include gelatin, agar, methylcellulose, starch, starch degradation products, and vinyl polymers. Curing agents encapsulated in protective polymers may be any material that reacts with epoxy groups. This includes amines, amino-containing polyamides, acids, and acid anhydrides.

The solid-in-oil-in-water (S/O/W) emulsion solvent evaporation technique¹⁰ employed in this work is widely used for microencapsulation because it is rather easy to scale up, as shown in the commercially available product Lupron Depot.^{11,12}

Many studies have been conducted to study the curing kinetics of epoxy resins with differential scanning calorimetry (DSC),^{13,14} isothermal DSC,¹⁵ Raman spectrometry,¹⁶ Fourier transform infrared (FTIR) analysis,¹⁷ and so on. Reports on the preparation of epoxy-resin-based systems with the addition of microencapsulated curing agents have been presented many times; however, the effects of microencapsulation on the curing behavior of epoxy resin systems are expounded quite rarely.

The objective of this study was to prepare 2-phenyl imidazole (2PZ)/poly(methyl methacrylate) (PMMA) microcapsules and apply them to epoxy resin systems as latent curing agents. The curing kinetics initiated by 2PZ and its microencapsulated congener were analyzed with a scanning DSC technique combined with Kissinger and Crane equations. Meanwhile, the curing mechanisms were also investigated with scanning DSC combined with FTIR studies.

EXPERIMENTAL

Materials

Curing agent 2PZ (98%), used as a core material, was purchased from Kaile Chemical Plant (Zhejiang, China). PMMA, used as a wall material, was supplied by Huadong Pharmaceutical Co. (Hangzhou, Zhejiang, China). Dichloromethane (DCM; a solvent) and sodium dodecyl sulfate (SDS; an emulsifier) were also supplied by Huadong Pharmaceutical.

Diglycidyl ether of bisphenol A (DGEBA; E-44), applied as a resin matrix, was purchased from Wujiang Heli Resin Plant (Jiangsu, China). All the reagents were analytical-grade without further purification.

Preparation of the PMMA microspheres

An oil-in-water emulsion was formed by the addition of a 50-mL aqueous solution containing 1 wt % SDS to 20 mL of DCM with 5 wt % PMMA at a vigorous stirring rate of 500 rpm to obtain a uniform liquid. Subsequently, the mixture was added to a 200-mL aqueous solution with 0.5 wt % SDS as a protective colloid. At the same time, the oil-in-water solution was heated to 30°C, approaching the boiling point of DCM at a rate of 2°C/min. DCM as a solvent was evaporated thoroughly from the surfaces of oily globules for more than 2 h to precipitate the PMMA microspheres. The obtained PMMA microspheres were washed with deionized water and then were filtered and dried in a vacuum oven at 40°C for at least 24 h.

Preparation of the 2PZ/PMMA microcapsules

2PZ (1 g) and PMMA (2 g) were dissolved in DCM (40 mL) as the dispersed phase, which was added to the continuous phase (1.5 wt % SDS in an aqueous solution, 50 mL) under high-speed agitation at room temperature for 30 min to get an S/O/W emulsion. Subsequently, the resultant S/O/W emulsion was poured into a 200-mL aqueous solution with 0.5 wt % SDS, and energetic agitation was continued. DCM was allowed to evaporate completely under the same conditions used for evaporation to prepare PMMA microspheres, and PMMA microcapsules containing the core material (2PZ) were obtained. The microcapsules were washed several times with deionized water and then dried.

Characterization of the microparticles

The diameter and surface morphology of the 2PZ/PMMA microcapsules and PMMA microspheres were observed with scanning electron microscopy (SEM; S-570, Hitachi). The specimens for SEM obser-

TABLE II
Samples b and c with Five Different Heating Histories
for Scanning DSC Studies Combined with FTIR

| Step | Heating history |
|------|--|
| 1 | Before curing |
| 2 | 110°C for 1.5 h |
| 3 | 110°C for 1.5 h and 130°C for 1.5 h |
| 4 | 110°C for 1.5 h, 130°C for 1.5 h, and 160°C for 1.5 h |
| 5 | 110°C for 1.5 h, 130°C for 1.5 h, 160°C for 1.5 h, and 250°C for 1.5 h |

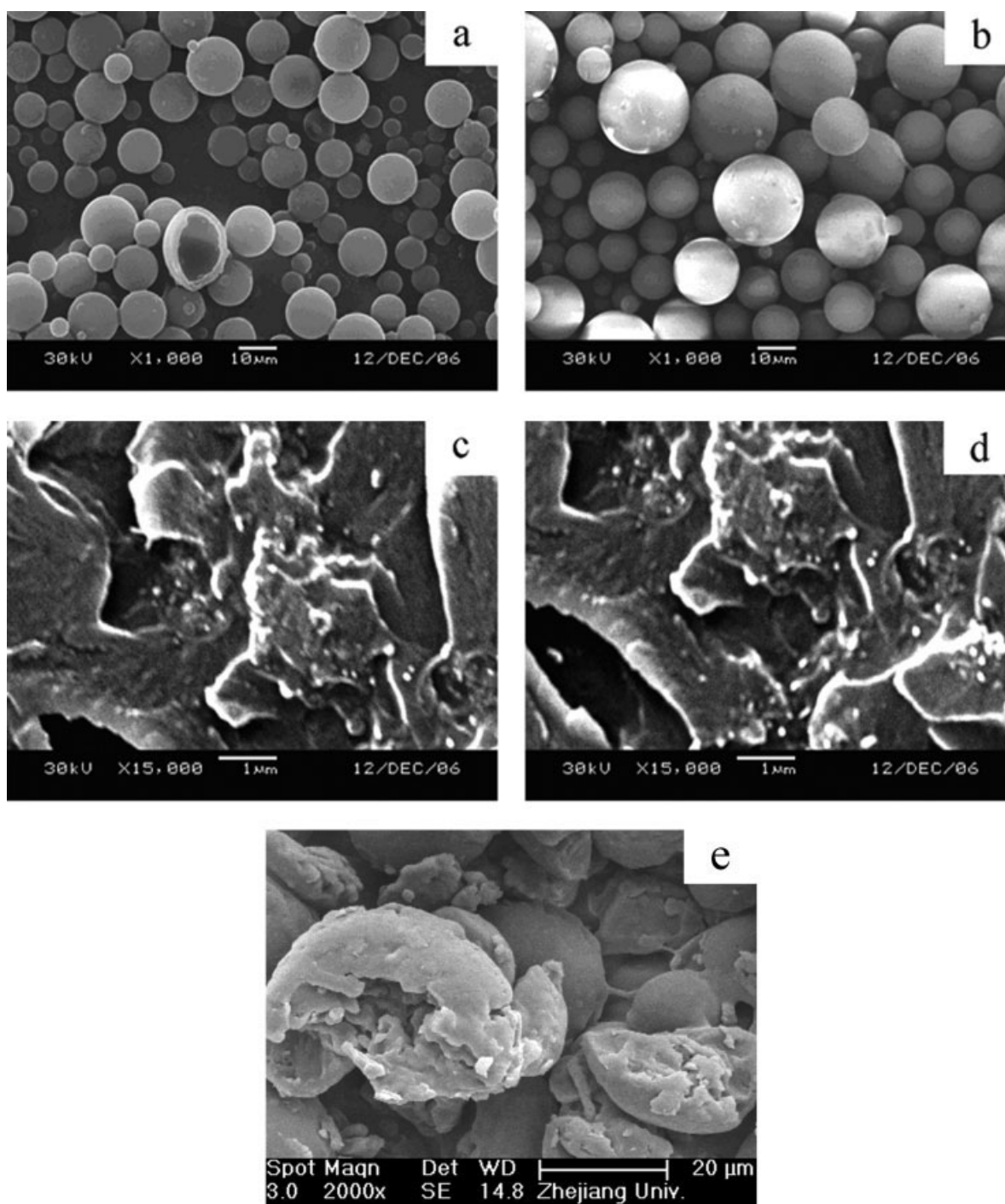


Figure 1 SEM micrographs of (a,c) PMMA microspheres, (b,d) 2PZ/PMMA microcapsules, and (e) pestled 2PZ/PMMA microcapsules.

vations were prepared through the equable spreading of particles on metal stubs fixed with double-sided conductive adhesive tape and coated with a thin gold film.

The 2PZ content of the microcapsules was measured with thermogravimetric analysis (TGA; Pyris 6, PerkinElmer). The samples were heated from room temperature to 600°C at a heating rate (β) of 20°C/min under a constant N₂ flow.

Characterization of the curing process for the epoxy resin

DSC studies were performed on a thermal analyzer (DSC Q100, TA, United States). The samples listed in Table I [(a) DGEBA/PMMA, (b) DGEBA/2PZ, (c) DGEBA/2PZ-PMMA microcapsules, and (d) DGEBA/2PZ/PMMA] were scanned at β values of 5, 10, and 20°C/min in an N₂ atmosphere. Scanning DSC stud-

ies, combined with FTIR (Vector 22, Bruker, Germany; KBr), were also carried out to study the cure of the DGEBA epoxy with 2PZ and 2PZ/PMMA microcapsules (Table I, samples b and c), which were heated under five different conditions called steps 1–5, as shown in Table II.

RESULTS AND DISCUSSION

Characterization of the prepared microparticles

The process of microencapsulation was performed because of the higher drug loading ratio and suitable particle size. The morphologies of the 2PZ/PMMA microcapsules and PMMA microspheres were characterized with SEM, as shown in Figure 1. Regular spheres of the 2PZ/PMMA microcapsules and PMMA microspheres with a well-proportioned size of about 10 μm were observed, and the PMMA microspheres were slightly smaller than the 2PZ/PMMA microcapsules. The surface of the microparticles was coarse and porous under a high magnification (15,000 \times). Besides, when the 2PZ/PMMA microcapsules were pestled and washed with glycol (a good solvent for 2PZ), a core–wall structure with thick walls and irregular small cores could be found with SEM, as shown in Figure 1(e).

The process of microencapsulation was performed because of the higher drug loading ratio and suitable particle size. The properties of the 2PZ/PMMA microcapsules and PMMA microspheres were characterized with TGA and SEM.

Figure 2 shows the TGA curves for 2PZ, 2PZ/PMMA microcapsules, and PMMA microspheres at $\beta = 20^\circ\text{C}/\text{min}$ under an N_2 atmosphere. 2PZ began to decompose at 155°C and decomposed completely at 280°C [Fig. 2(a)]; meanwhile, PMMA microspheres started and ended decomposition at 350 and 450°C , respectively [Fig. 2(c)]. The TGA curve of the 2PZ/PMMA microcapsules [Fig. 2(b)] exhibits two steps: the first one appears at about 210°C because of the decomposition of 2PZ, and the other one, at about 360°C , is mainly attributable to the decomposition of PMMA polymeric walls. An obvious delay in the decomposition for 2PZ in microcapsules versus that for pure 2PZ [Fig. 2(a)] was observed because of the protection of the PMMA polymeric wall, which absorbed a large quantity of melting heat and resulted in the retarded decomposition of 2PZ at nearly 60°C . We think that 2PZ decomposed almost completely when PMMA began to decompose [Fig. 2(b)] because the temperature span of 2PZ from the beginning of weight loss to full decomposition [Fig. 2(a)], about 120°C , was equal to that of sample b [Fig. 2(b)]. Therefore, the weight loss until the second step was supposed to be the weight of 2PZ contained in the 2PZ/PMMA microcapsules. Calculated

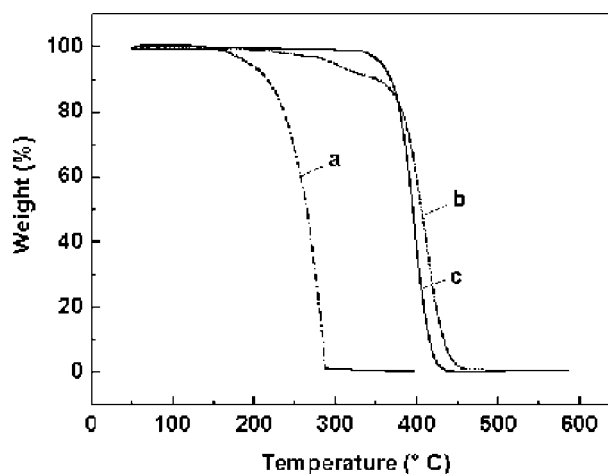


Figure 2 TGA curves for the residual weights of (a) 2PZ, (b) 2PZ/PMMA microcapsules, and (c) PMMA microspheres at $\beta = 20^\circ\text{C}/\text{min}$ under an N_2 flow.

from Figure 2(b), the concentration of 2PZ in the microcapsules was about 10 wt %. The decomposition temperature of PMMA in Figure 2(b) shifted to a higher value than that in Figure 2(c), and this was probably caused by remnants of the earlier decomposed 2PZ in the 2PZ/PMMA microcapsules. What remained on the surface of PMMA delayed the decomposition process of PMMA and led to a higher decomposition temperature.

Effect of microencapsulation on the curing kinetics

DSC studies of four epoxy resin systems, to which PMMA microspheres, 2PZ, 2PZ/PMMA microcapsules, and a mixture of 2PZ and PMMA microspheres were added, were carried out to determine the effect of the addition of microencapsulated latent curing agents on the curing kinetics of epoxy resin systems. The constituents of the samples studied with scanning DSC are listed in Table I, and the DSC curves and the data are given in Figure 3 and Table III, respectively. A flat and nearly smooth trend can be observed in Figure 3(a), which confirms that the PMMA microspheres were unable to cause a curing reaction of the epoxy resin, and no self-curing reaction of the epoxy resin was initiated during the whole process. As for the other curves in Figure 3, two exothermal peaks of the curing reaction can be detected around 130 and 230°C . The effect of the PMMA microspheres on the initiation temperature is not obvious for the values of the approaching onset cure temperature (T_0) in Figure 3(b,d), which are 89.68 and 93.93°C (Table III), respectively.

The reaction heat for the first peak (ΔH_1) of sample d was smaller than that for sample b because of the curing reaction heat absorbed partly by the endothermic melting process of the PMMA micro-

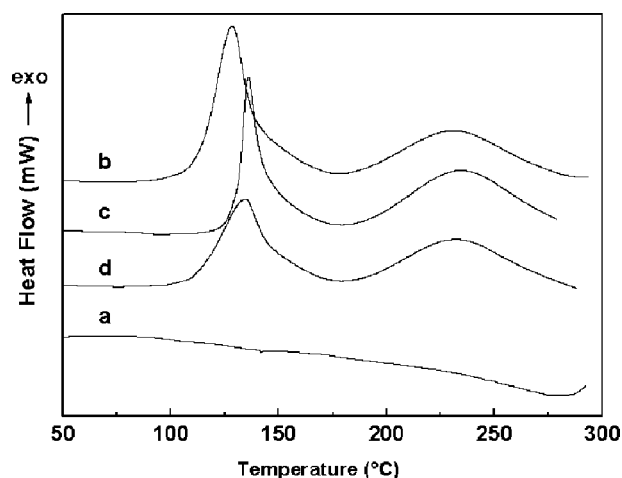
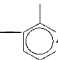


Figure 3 Scanning DSC curves of samples a–d at $\beta = 5^\circ\text{C}/\text{min}$.

spheres: its softening temperature was about 118°C . To exclude the effect of the crosslinking degree of the epoxy resin on ΔH_1 , the concentrations of residual epoxide groups in samples b–d, which were heated from 50 to 180°C at $\beta = 5^\circ\text{C}/\text{min}$ in the DSC apparatus, were detected by FTIR analysis, as shown in Figure 4. With the absorption peak of aromatic rings (phenyl—, an absorption band near 830 cm^{-1})

as an internal standard, residual epoxide groups in the three samples were calculated by the division of the area of the absorption peak by the absorption peak of the aromatic rings. The ratios of the three samples were 0.108, 0.103, and 0.099, respectively, and this means that the residual epoxide groups in the three samples were almost the same after the first curing reaction; that is, the crosslinking degrees of the three samples after the first reaction were similar. The first peak of sample c shifted toward a higher temperature, and the width of the peak was narrower in comparison with those of sample b because of the protection of the PMMA polymeric walls for 2PZ and the endothermic melting process of the PMMA walls, respectively, which can be determined clearly from the data listed in Table III. Xing et al.⁴ also pointed out that the entrapment of curing agents protects them from a curing reaction

TABLE III
 T_o , T_p , and ΔH Values of Two Exothermic Peaks for Samples b–d Obtained by Scanning DSC at $\beta = 5^\circ\text{C}/\text{min}$ Under N_2

| Sample | T_o ($^\circ\text{C}$) | T_{p1} ($^\circ\text{C}$) | T_{p2} ($^\circ\text{C}$) | ΔH_1 (J/g) | ΔH_2 (J/g) |
|--------|----------------------------|-------------------------------|-------------------------------|--------------------|--------------------|
| b | 89.68 | 128.66 | 231.29 | 271.10 | 188.39 |
| c | 118.39 | 140.05 | 233.69 | 198.97 | 191.75 |
| d | 93.93 | 134.69 | 232.82 | 210.65 | 190.48 |

Subscripts 1 and 2 refer to the first and second exothermic peaks, respectively.

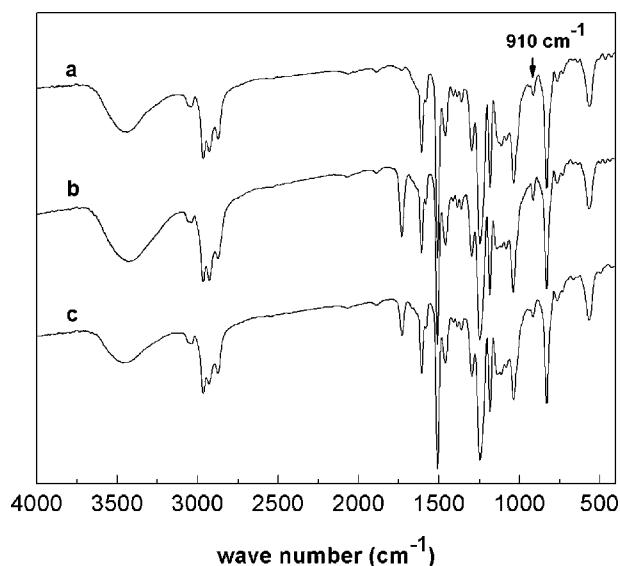


Figure 4 FTIR spectra of (a) sample b, (b) sample c, and (c) sample d heated from 50 to 180°C at $\beta = 5^\circ\text{C}/\text{min}$ in the DSC apparatus.

in storage and delays the curing procedure in comparison with systems with unentrapped curing agents when the curing reaction starts. We think that the barrier action of PMMA between epoxy and 2PZ in sample d was partial in comparison with that of the embedded polymeric containers in sample c because of the independent dispersion of PMMA and 2PZ in the epoxy resin matrix. Therefore, the first peak temperature (T_{p1}) of sample d was between those of samples b and c. The values of the reaction heat and peak temperature of the second peak (ΔH_2 and T_{p2}) determined for the three samples are given in Table III, and no obvious change took place.

The cure kinetics were studied with dynamic experiments at different values of β and applied to the Kissinger method,¹⁸ which is given by the following equation:

TABLE IV
Thermodynamic Parameters Obtained from the Exothermic Peaks of Scanning DSC Curves at Different Values of β for Samples b–d

| Sample | β ($^\circ\text{C}/\text{min}$) | T_{p1} (K) | T_{p2} (K) |
|--------|---|--------------|--------------|
| b | 5 | 401.81 | 504.44 |
| | 10 | 414.42 | 517.93 |
| | 20 | 429.04 | 537.11 |
| c | 5 | 416.20 | 505.97 |
| | 10 | 424.77 | 516.83 |
| | 20 | 439.09 | 528.47 |
| d | 5 | 407.84 | 512.54 |
| | 10 | 417.08 | 522.83 |
| | 20 | 431.73 | 533.37 |

Subscripts 1 and 2 refer to the first and second peaks, respectively.

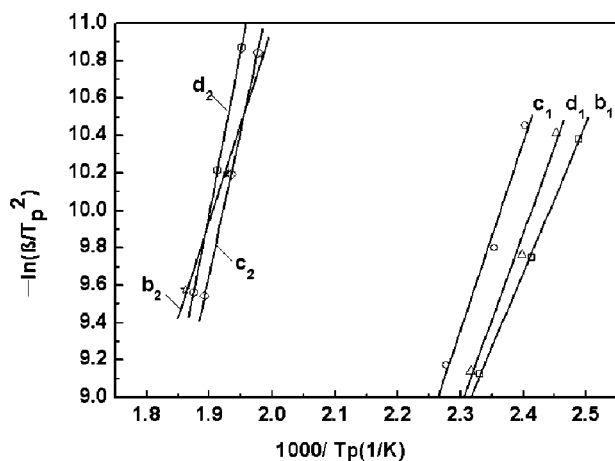


Figure 5 Relationship of $-\ln(\beta/T_p^2)$ and $1000/T_p$ for samples b–d. Subscripts 1 and 2 refer to the first and second exothermal peaks, respectively.

$$\frac{d(\ln \beta/T_p^2)}{d(1/T_p)} = -\frac{E_a}{R} \quad (1)$$

where E_a is the activation energy, T_p is the peak exothermal temperature, and R is the gas constant. E_a can be calculated from the slope of the plot of $-\ln(\beta/T_p^2)$ versus $1000/T_p$. The Crane method,¹⁹ as depicted in Eq. (2), was applied as well to obtain the curing reaction order (n):

$$\frac{d(\ln \beta)}{d(1/T_p)} = -\left[\frac{E_a}{nR} + 2T_p\right] \approx -\frac{E_a}{nR} \quad (2)$$

To detect the effects of the curing agents in samples b–d on the reactivities toward the epoxy resins, the cure kinetics of samples b–d were examined with a dynamic DSC technique at β values of 5, 10, and 20°C/min; the analyzed data are given in Table IV.

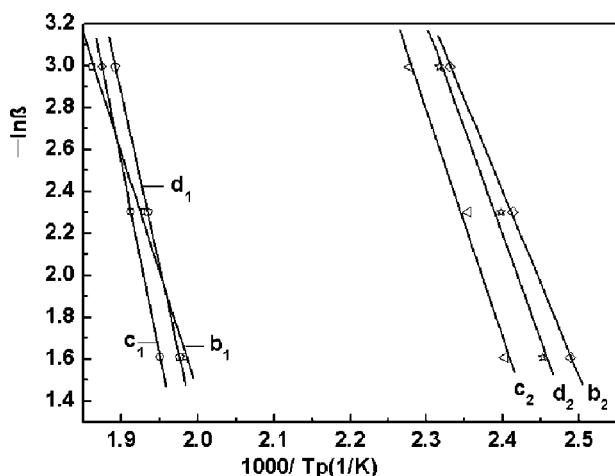


Figure 6 Relationship of $-\ln \beta$ and $1000/T_p$ for samples b–d. Subscripts 1 and 2 refer to the first and second exothermal peaks, respectively.

TABLE V
 E_a and n Values of Samples b–d

| Sample | E_{a1} (kJ/mol) | E_{a2} (kJ/mol) | n_1 | n_2 |
|--------|-------------------|-------------------|-------|-------|
| b | 66.04 | 98.51 | 0.91 | 0.91 |
| c | 89.36 | 104.73 | 0.93 | 0.94 |
| d | 76.84 | 101.60 | 0.92 | 0.94 |

Subscripts 1 and 2 refer to the first and second peaks, respectively.

T_o , T_{p1} , and T_{p2} of all the samples shifted toward a higher temperature with an increase in β . The correspondence of $-\ln(\beta/T_p^2)$ and $1000/T_p$ is presented in Figure 5. From the slope of the straight lines and Kissinger equation, E_a was calculated, and in the same way, n was obtained from the slope of the plot of $-\ln \beta$ versus $1000/T_p$ (in Fig. 6) in combination with the Crane equation. The E_a and n values are listed in Table V. E_{a1} of sample c was higher than those of samples b and d (ca. 20 and 10 kJ/mol, respectively), whereas the E_{a2} values of the three samples were basically accordant. The conclusion can be drawn that the increased E_{a1} value was caused by the addition of the microencapsulated curing agents to the epoxy resin system, which had little effect on E_{a2} in all three samples. The increased E_{a1} value of sample c revealed the nature of the curing reaction delayed by microencapsulation, and it matched the higher T_o value adapted for storage for a long time at room temperature. The values of another curing kinetic parameter, n , of samples b and c, calculated from the slopes of the Crane relationship for the epoxy resin systems, were quite close, and this means that the curing reactions of the two samples proceeded conformably. A contrastive experiment of samples b and c for deposition was carried out to determine their stability in storage. Sample b was cured after 7 days, whereas sample c

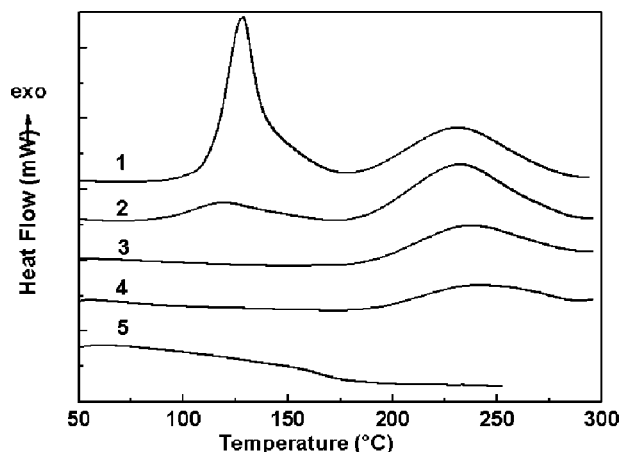


Figure 7 Scanning DSC curves of sample b undergoing five different heating histories defined in Table II at $\beta = 5^\circ\text{C}/\text{min}$ under an N_2 flow.

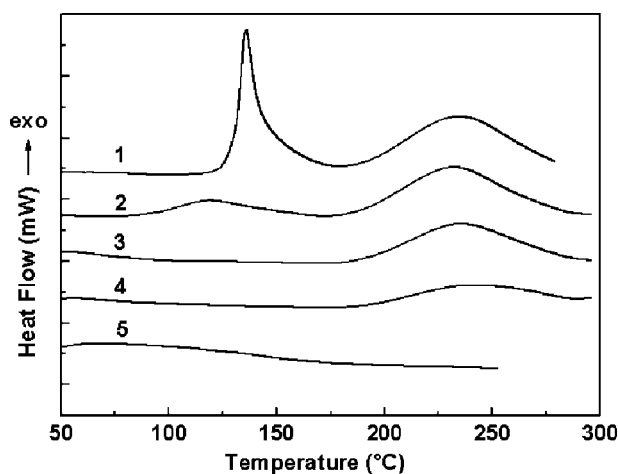


Figure 8 Scanning DSC curves of sample c undergoing five different heating histories defined in Table II at $\beta = 5^\circ\text{C}/\text{min}$ under an N_2 flow.

was still fluid even after being kept for more than 3 months at room temperature.

From the values of T_o , T_p , ΔH , and E_a mentioned previously, it can be concluded that 2PZ displays higher reactivity and releases more heat during the curing process than its microencapsulated parallel, and this means that microencapsulated curing agents participate with more difficulty in curing reactions and are more stable in epoxy resins during storage for protective container effects of PMMA walls around 2PZ. The addition of PMMA microspheres to the DGEBA/2PZ system makes the cure reactivity decrease for the barrier effect between the epoxy resin and 2PZ.

Effect of microencapsulation on the curing mechanism

The curing mechanisms of samples b and c were studied with a scanning DSC technique. The curing behaviors of DGEBA/2PZ and DGEBA/2PZ-PMMA microcapsules (Table I, samples b and c) undergoing five different heating histories (steps 1–5 in Table II) were studied with scanning DSC and FTIR. Figure 7 shows the DSC curves of sample b undergoing five different heating histories. In Figure 7, two exothermal peaks can be distinguished in curves 1 and 2,

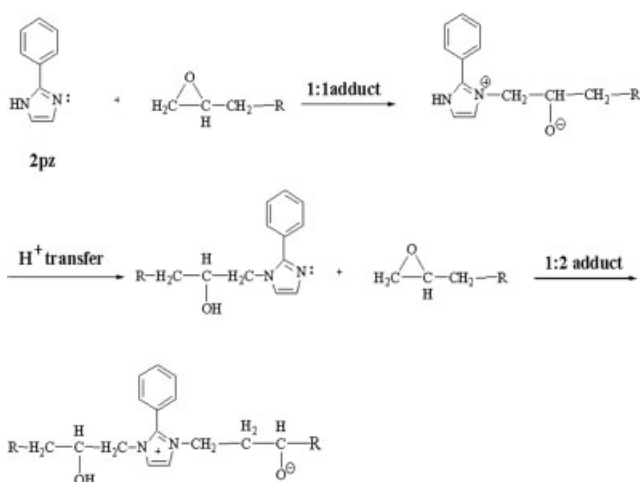
and the first exothermal peak becomes much flatter, but the second one shows no obvious change after the heating of the sample at 110°C for 1.5 h. However, after the heating of the sample at 130 and 160°C for 1.5 h, respectively [Fig. 7(3,4)], the first peak disappears, and the second one becomes more and more feeble and finally vanishes [Fig. 7(5)]. Figure 8 displays scanning DSC curves of sample c under five different heating histories, and the same trend revealed in Figure 7 is exhibited. Meanwhile, the glass-transition temperature (T_g) values of completely cured samples b and c, determined by DSC curves [Figs. 7(5) and 8(5)], were 165.20 and 142.11°C . T_g of sample b, which was a bit higher than that reported by Ooi et al.²⁰ (the highest was 154°C), was nearly 20°C higher than that of c, probably because of the addition of PMMA, which can be used to increase the toughness of cured epoxy polymers because of its flexible molecular chain. ΔH_1 and ΔH_2 (Figs. 7 and 8) are listed in Table VI.

A curing mechanism of DGEBA/2PZ is proposed that is based on the work of Ooi et al.²⁰ and Barton and Shepherd,²¹ and a sketch of the curing mechanism of DGEBA/2PZ is given in Schemes 1 and 2. The formation of the 1 : 1 adduct is generated through an attack on the epoxy-functional group of DGEBA by the more basic pyridine-type nitrogen ($-\text{N}-$) of 2PZ. Then, the newly generated pyridine-type nitrogen attacks another epoxy group to produce the 1 : 2 adduct (Scheme 1). In the second step, these generated adducts are assumed to act as the initiators for the polymerization of DGEBA by an etherification reaction in which the reactive alkoxide anion is the propagating species (Scheme 2). Ooi et al. also reported that two exothermal peaks could be observed in 2PZ curing systems; the first peak was assigned to adduct formation, whereas the second one was due to alkoxide-initiated polymerization. The first peaks in Figures 7(2) and 8(2), much flatter than those in Figures 7(1) and 8(1), are due to adducts generated by the consumption of 2PZ after heating. When 2PZ is exhausted, the first reaction step (Scheme 1) is over, and the first peaks attributable to the first step disappear in Figures 7(3) and 8(3). As the samples are heated subsequently, the second reaction step (Scheme 2) takes place, and it

TABLE VI
 ΔH Values of Samples b and c Undergoing Five Different Heating Histories Depicted by Scanning DSC at $\beta = 5^\circ\text{C}/\text{min}$ Under N_2

| | Sample b | | | | | Sample c | | | | |
|--------------------|----------|--------|--------|-------|---|----------|--------|--------|-------|---|
| | 1 | 2 | 3 | 4 | 5 | 1 | 2 | 3 | 4 | 5 |
| ΔH_1 (J/g) | 271.10 | 35.64 | 0 | 0 | 0 | 198.97 | 40.88 | 0 | 0 | 0 |
| ΔH_2 (J/g) | 188.39 | 160.54 | 118.85 | 70.05 | 0 | 191.75 | 161.42 | 141.31 | 91.33 | 0 |

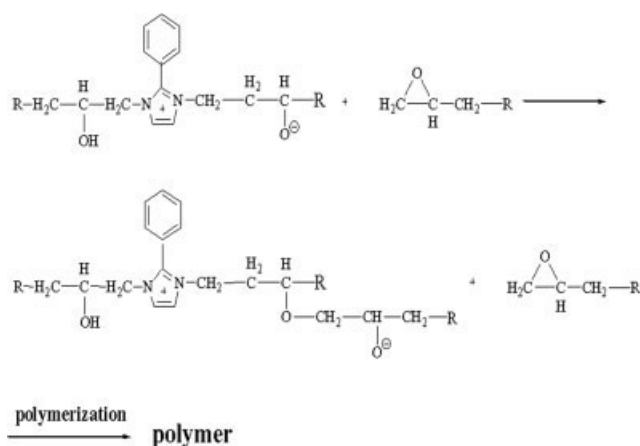
Subscripts 1 and 2 refer to the first and second peaks, respectively.



Scheme 1 Proposed adduct formation of the DGEBA epoxy resin.

results in the second peak area decreasing and vanishing at last, as shown in Figures 7(3–5) and 8(3–5). According to the mechanism mentioned previously, 2PZ is not involved in the second curing reaction step of a DGEBA epoxy resin; therefore, the second peak areas for all samples illuminated in Figure 3 are coherent for the exhaustion of 2PZ in adduct formation and its absence in alkoxide-initiated polymerization.

To obtain more evidence on the effects of microencapsulation on the curing reactions of DGEBA epoxy resin systems, FTIR studies were also performed on samples b and c undergoing five different heating histories, as defined in Table II, and FTIR spectra are shown in Figures 9 and 10, respectively. The absorption peaks near 3460 and 910 cm^{-1} are assigned to hydroxyl ($-OH$) and epoxide groups ($\begin{matrix} H_2C \\ \diagup \quad \diagdown \\ O \end{matrix}$), respectively. The hydroxyl peak at 3460 cm^{-1} intensifies with the progression of the heating treatment



Scheme 2 Proposed alkoxide-initiated polymerization of the DGEBA epoxy resin.

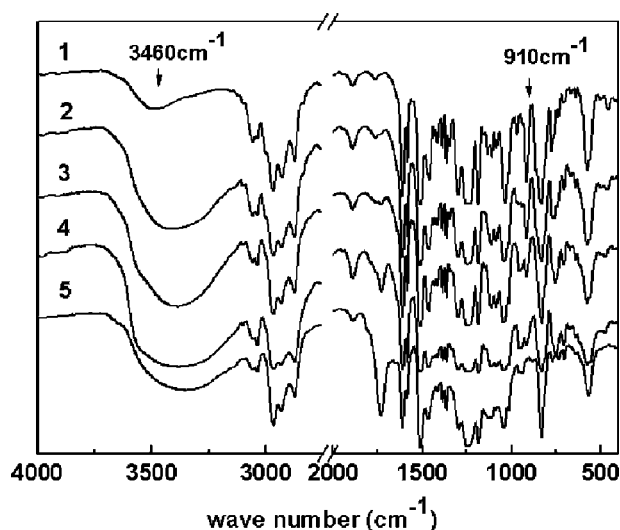


Figure 9 FTIR spectra of sample b undergoing five different heating histories.

[Figs. 9(1)–(3) and 10(1)–(3)] and retains its coherence when the adduct reaction is over [Figs. 9(4,5) and 10(4,5)]. Moreover, the peaks of the epoxide group at 910 cm^{-1} decrease and finally disappear from 1 to 5 in Figures 9 and 10 for the consumption of epoxide groups. These conclusions agree with those drawn from Figures 7 and 8.

We think that microencapsulated curing agents do not cause a change in the curing mechanism for epoxy resins because the trends of samples b and c in Figures 7 and 8 are the same.

More proof about the conformability of the curing mechanism for samples b and c can be collected by the quantification of the concentration of epoxide-functional groups. Because aromatic rings (phenyl- an absorption band near 830 cm^{-1}) do not

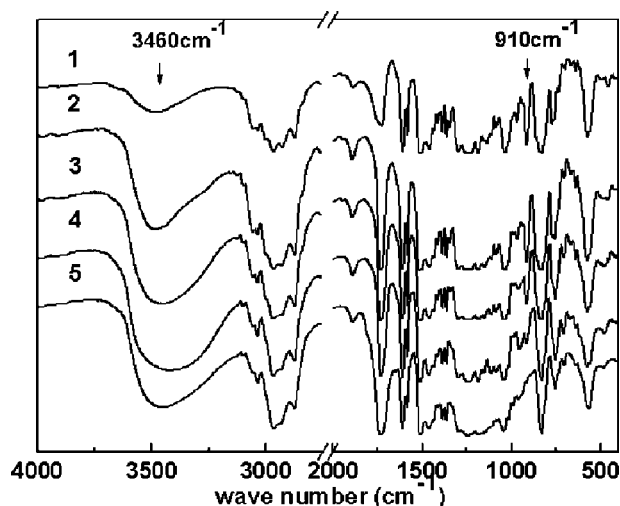


Figure 10 FTIR spectra of sample c undergoing five different heating histories.

TABLE VII
Normalized FTIR Absorption Ratio Data for Samples b
and c Undergoing Five Different Heating Histories

| Sample | $A_n(t)^*$ | | | | |
|--------|----------------|----------------|----------------|----------------|----------------|
| | Heating step 1 | Heating step 2 | Heating step 3 | Heating step 4 | Heating step 5 |
| b | 1.00 | 0.77 | 0.50 | 0.26 | 0 |
| c | 1.00 | 0.74 | 0.50 | 0.24 | 0 |

change during the curing reaction, their absorption peak can be used as an internal standard for sample b. As for sample c, core material 2PZ, having aromatic rings, is encapsulated by PMMA polymeric walls, and this results in changes in the concentration of aromatic rings during the thermal curing procedure when PMMA polymeric walls melt and liberate 2PZ in an epoxy resin matrix. Carbonyl (1692 cm^{-1} , versus, $>\text{C}=\text{O}$) was chosen as an internal standard for sample c. The absorption peak of the characterized epoxide-functional group with time [$A_n(t)$] was then normalized by its division by the absorption peak of the aromatic rings (or carbonyl) with time [$A_{\text{ref}}(t)$]. The normalized absorption with time [$A_n(t)^*$] was determined as follows:

$$A_n(t)^* = A_n(t)/A_{\text{ref}}(t) \quad (3)$$

The reactivities of 2PZ and 2PZ/PMMA microcapsules with the epoxy resin during the curing process can be viewed through the normalized absorption changes of the characterized epoxide-functional groups with time. The ratios of the normalized absorption peaks of the epoxide-functional group at various times during the cure period previously described are listed in Table VII, which illuminates the conformable consumption scope of the epoxide groups during the five heating steps for samples b and c; the conformability of the curing reaction is revealed as well.

CONCLUSIONS

The solvent evaporation method was applied to prepare 2PZ/PMMA microcapsules, in which the concentration of 2PZ was 10 wt %, as determined by TGA. Regular spherical microcapsules and PMMA microspheres with a well-proportioned size of about $10\text{ }\mu\text{m}$ were characterized with SEM.

T_o and T_p of a DGEBA/2PZ-PMMA microcapsule system, determined with scanning DSC, appeared to shift nearly 10°C higher than those of a DGEBA/2PZ system because of the increased reaction energies of curing (E_a), and this was attributed to microencapsulation of the curing agents. The decreased value of ΔH_1 was due to the endothermic melting procedure of PMMA embedded in an epoxy resin matrix. The

increased reaction energies for the cure of the DGEBA/2PZ-PMMA microcapsule system made it more suitable for storage. DGEBA/2PZ was cured after 7 days, whereas the DGEBA/2PZ-PMMA microcapsule system was still fluid even after more than 3 months at room temperature. The n values of the employed systems were quite close, and this shows that the curing reactions of the two samples proceeded conformably and that microencapsulation may not influence curing reactions of DGEBA.

The proposed curing mechanism for the 2PZ curing epoxy resin can explain the phenomenon perfectly. Data obtained from FTIR, combined with scanning DSC studies, for DGEBA/2PZ and DGEBA/2PZ-PMMA microcapsules undergoing five different heating histories showed that no obvious mechanical change occurred when the curing agents were replaced by 2PZ/PMMA microcapsules. T_g of the DGEBA/2PZ system was 165.20°C , nearly 20°C higher than that of the system of DGEBA/2PZ-PMMA microcapsules, and this could probably be attributed to the addition of PMMA, which can be used to increase the toughness of cured epoxy resin systems because of its flexible molecular chain.

References

- Lubin, G. Handbook of Composites; Van Nostrand Reinhold: New York, 1982.
- Chen, Y.; Chiu, W.; Lin, K. J Polym Sci Part A: Polym Chem 1999, 37, 3233.
- Xu, K.; Chen, M.; Zhang, K.; Hu, J. Polymer 2004, 45, 1133.
- Xing, S.; Wang, Z.; Zeng, J. J Natl Univ Defense Technol 2006, 28, 31.
- Noro, H.; Fusumada, M. (to Nitto Denko Corp.). U.S. Pat. 6,916,538 (2005).
- Cao, M.; Xie, P.; Jin, Z. J Appl Polym Sci 2000, 85, 873.
- Bohli, W. H. (to the United States of America). U.S. Pat. 3,866,873 (1975).
- Brandys, F. A.; Irwin, M. J. (to 3M Innovative Properties Co.). U.S. Pat. 6,506,494 (2003).
- Meier, D. J.; Kahn, A. (to Shell Oil Co.). U.S. Pat. 3,018,258 (1962).
- Takada, S.; Yamagata, Y.; Misaki, M.; Taira, K.; Kurokawa, T. J Controlled Release 2003, 88, 229.
- Ogawa, Y.; Yamamoto, M.; Takada, S.; Okada, H.; Shimamoto, T. Chem Pharm Bull 1988, 36, 1502.
- Okada, H.; Doken, Y.; Ogawa, Y.; Toguchi, H. Pharm Res 1994, 11, 1143.
- Choi, E. J.; Seo, J. C.; Bae, H. K. Eur Polym 2004, 40, 256.
- Assche, G. V.; Hemelrijck, A. V.; Rahier, H. Thermochim Acta 1996, 286, 209.
- Lee, J. L.; Choi, H. K.; Shim, M. J. Thermochim Acta 2000, 343, 111.
- Rocks, J.; Rintoul, L.; Vohwinkel, F. Polymer 2004, 45, 6799.
- Scherzer, T.; Decker, U. Polymer 2000, 41, 7681.
- Kissinger, H. E. Anal Chem 1957, 29, 1702.
- Crane, L. W.; Dynes, P. J.; Kaelble, D. H. J Polym Sci 1973, 11, 533.
- Ooi, S. K.; Cook, W. D.; Simon, G. P.; Such, C. H. Polymer 2000, 41, 3639.
- Barton, J. M.; Shepherd, P. M. Makromol Chem 1975, 176, 919.